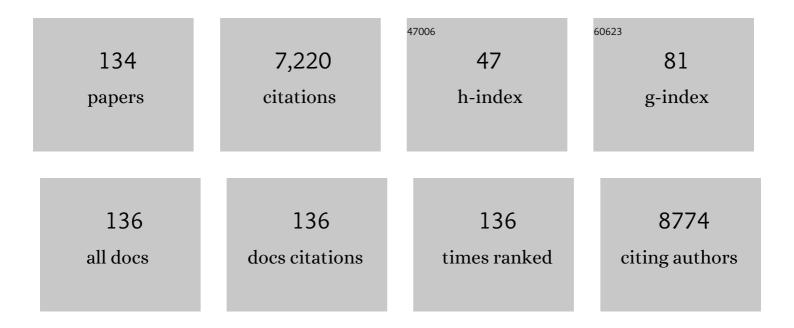
List of Publications by Year in descending order

Source: https://exaly.com/author-pdf/705820/publications.pdf Version: 2024-02-01



OSKAD DADIS

#	Article	IF	CITATIONS
1	A reconsideration of the relationship between the crystallite size La of carbons determined by X-ray diffraction and Raman spectroscopy. Carbon, 2006, 44, 3239-3246.	10.3	452
2	Mapping amorphous calcium phosphate transformation into crystalline mineral from the cell to the bone in zebrafish fin rays. Proceedings of the National Academy of Sciences of the United States of America, 2010, 107, 6316-6321.	7.1	389
3	Decomposition and carbonisation of wood biopolymers—a microstructural study of softwood pyrolysis. Carbon, 2005, 43, 53-66.	10.3	279
4	A customizable software for fast reduction and analysis of large X-ray scattering data sets: applications of the new <i>DPDAK</i> package to small-angle X-ray scattering and grazing-incidence small-angle X-ray scattering. Journal of Applied Crystallography, 2014, 47, 1797-1803.	4.5	244
5	Continuous Structural Evolution of Calcium Carbonate Particles:Â A Unifying Model of Copolymer-Mediated Crystallization. Journal of the American Chemical Society, 2007, 129, 3729-3736.	13.7	240
6	Bone mineralization in an osteogenesis imperfecta mouse model studied by small-angle x-ray scattering Journal of Clinical Investigation, 1996, 97, 396-402.	8.2	203
7	Influence of coherency stress on microstructural evolution in model Ni-Al-Mo alloys. Acta Metallurgica Et Materialia, 1995, 43, 1007-1022.	1.8	168
8	Infrared Emitting and Photoconducting Colloidal Silver Chalcogenide Nanocrystal Quantum Dots from a Silylamide-Promoted Synthesis. ACS Nano, 2011, 5, 3758-3765.	14.6	164
9	The grinding tip of the sea urchin tooth exhibits exquisite control over calcite crystal orientation and Mg distribution. Proceedings of the National Academy of Sciences of the United States of America, 2009, 106, 6048-6053.	7.1	161
10	A new experimental station for simultaneous X-ray microbeam scanning for small- and wide-angle scattering and fluorescence at BESSY II. Journal of Applied Crystallography, 2006, 40, s466-s470.	4.5	148
11	Microtexture and Chitin/Calcite Orientation Relationship in the Mineralized Exoskeleton of the American Lobster. Advanced Functional Materials, 2008, 18, 3307-3314.	14.9	145
12	Tracking the structural arrangement of ions in carbon supercapacitor nanopores using in situ small-angle X-ray scattering. Energy and Environmental Science, 2015, 8, 1725-1735.	30.8	126
13	Imaging of the helical arrangement of cellulose fibrils in wood by synchrotron X-ray microdiffraction. Journal of Applied Crystallography, 1999, 32, 1127-1133.	4.5	123
14	Novel Insights into Nanopore Deformation Caused by Capillary Condensation. Physical Review Letters, 2008, 101, 086104.	7.8	110
15	Insights into the chemical composition of Equisetum hyemale by high resolution Raman imaging. Planta, 2008, 227, 969-980.	3.2	109
16	Strontium is incorporated into mineral crystals only in newly formed bone during strontium ranelate treatment. Journal of Bone and Mineral Research, 2010, 25, 968-975.	2.8	108
17	On the mineral in collagen of human crown dentine. Biomaterials, 2010, 31, 5479-5490.	11.4	106
18	Nanoporous activated carbon cloth as a versatile material for hydrogen adsorption, selective gas separation and electrochemical energy storage. Nano Energy, 2017, 40, 49-64.	16.0	101

#	Article	IF	CITATIONS
19	Physisorbed films in periodic mesoporous silica studied byin situsynchrotron small-angle diffraction. Physical Review B, 2006, 73, .	3.2	100
20	Early stages of precipitate rafting in a single crystal NiAlMo model alloy investigated by small-angle X-ray scattering and TEM. Acta Materialia, 1997, 45, 1085-1097.	7.9	98
21	Glucan, water dikinase phosphorylates crystalline maltodextrins and thereby initiates solubilization. Plant Journal, 2008, 55, 323-334.	5.7	94
22	Capillarity-driven deformation of ordered nanoporous silica. Applied Physics Letters, 2009, 95, 083121.	3.3	89
23	Texture of PAN- and pitch-based carbon fibers. Carbon, 2002, 40, 551-555.	10.3	86
24	Salt concentration and charging velocity determine ion charge storage mechanism in nanoporous supercapacitors. Nature Communications, 2018, 9, 4145.	12.8	85
25	Confinement-induced structural changes of water studied by Raman scattering. Physical Review B, 2011, 84, .	3.2	80
26	Biomimetics and Biotemplating of Natural Materials. MRS Bulletin, 2010, 35, 219-225.	3.5	79
27	Oriented aggregation of calcium silicate hydrate platelets by the use of comb-like copolymers. Soft Matter, 2013, 9, 4864.	2.7	78
28	Stiffness gradients in vascular bundles of the palm <i>Washingtonia robusta</i> . Proceedings of the Royal Society B: Biological Sciences, 2008, 275, 2221-2229.	2.6	77
29	Density minimum of confined water at low temperatures: a combined study by small-angle scattering of X-rays and neutrons. Physical Chemistry Chemical Physics, 2012, 14, 3852.	2.8	76
30	On the Stability of Amorphous Minerals in Lobster Cuticle. Advanced Materials, 2009, 21, 4011-4015.	21.0	74
31	Pore Structure and Fluid Sorption in Ordered Mesoporous Silica. I. Experimental Study by in situ Small-Angle X-ray Scattering. Journal of Physical Chemistry C, 2009, 113, 15201-15210.	3.1	74
32	Elastic moduli of nanocrystallites in carbon fibers measured by in-situ X-ray microbeam diffraction. Carbon, 2003, 41, 563-570.	10.3	72
33	Adsorption of n-Pentane on Mesoporous Silica and Adsorbent Deformation. Langmuir, 2013, 29, 8601-8608.	3.5	71
34	From diffraction to imaging: New avenues in studying hierarchical biological tissues with x-ray microbeams (Review). Biointerphases, 2008, 3, FB16-FB26.	1.6	70
35	Direct Observation of Nanocrystallite Buckling in Carbon Fibers under Bending Load. Physical Review Letters, 2005, 95, 225501.	7.8	69
36	Effect of particle size and Debye length on order parameters of colloidal silica suspensions under confinement. Soft Matter, 2011, 7, 10899.	2.7	69

#	Article	IF	CITATIONS
37	Hierarchical Calcite Crystals with Occlusions of a Simple Polyelectrolyte Mimic Complex Biomineral Structures. Advanced Functional Materials, 2012, 22, 4668-4676.	14.9	69
38	Hierarchically Structured Ceramics by High-Precision Nanoparticle Casting of Wood. Small, 2006, 2, 994-998.	10.0	68
39	Scanning texture analysis of lamellar bone using microbeam synchrotron X-ray radiation. Journal of Applied Crystallography, 2007, 40, 115-120.	4.5	68
40	The Two Plastidial Starch-Related Dikinases Sequentially Phosphorylate Glucosyl Residues at the Surface of Both the A- and B-Type Allomorphs of Crystallized Maltodextrins But the Mode of Action Differs. Plant Physiology, 2009, 150, 962-976.	4.8	67
41	In situ X-ray diffraction investigation of thermal decomposition of wood cellulose. Journal of Analytical and Applied Pyrolysis, 2007, 80, 134-140.	5.5	65
42	The Use of Smallâ€Angle Xâ€Ray Diffraction Studies for the Analysis of Structural Features in Archaeological Samples. Archaeometry, 2001, 43, 117-129.	1.3	64
43	The implication of chemical extraction treatments on the cell wall nanostructure of softwood. Cellulose, 2008, 15, 407.	4.9	64
44	Skin-core structure and bimodal Weibull distribution of the strength of carbon fibers. Carbon, 2007, 45, 2801-2805.	10.3	60
45	Pole figure analysis of mineral nanoparticle orientation in individual trabecula of human vertebral bone. Journal of Applied Crystallography, 2003, 36, 494-498.	4.5	54
46	Scanning X-ray imaging with small-angle scattering contrast. Journal of Applied Crystallography, 2007, 40, s78-s82.	4.5	54
47	Evaluation of 3D small-angle scattering from non-spherical particles in single crystals. Journal of Applied Crystallography, 1993, 26, 820-826.	4.5	51
48	Moistureâ€Ðriven Ceramic Bilayer Actuators from a Biotemplating Approach. Advanced Materials, 2016, 28, 5235-5240.	21.0	48
49	Isolation of Mesoporous Biogenic Silica from the Perennial Plant <i>Equisetum hyemale</i> . Chemistry of Materials, 2008, 20, 2020-2025.	6.7	47
50	Adsorption-Induced Deformation of Hierarchically Structured Mesoporous Silica—Effect of Pore-Level Anisotropy. Langmuir, 2017, 33, 5592-5602.	3.5	47
51	Structural and analytical studies of silica accumulations in Equisetum hyemale. Analytical and Bioanalytical Chemistry, 2007, 389, 1249-1257.	3.7	46
52	Scanning small-angle X-ray scattering analysis of the size and organization of the mineral nanoparticles in fluorotic bone using a stack of cards model. Journal of Applied Crystallography, 2010, 43, 1385-1392.	4.5	45
53	Surfactant Self-Assembly in Cylindrical Silica Nanopores. Journal of Physical Chemistry Letters, 2010, 1, 1442-1446.	4.6	45
54	Crystal Phase Transitions in the Shell of PbS/CdS Core/Shell Nanocrystals Influences Photoluminescence Intensity. Chemistry of Materials, 2014, 26, 5914-5922.	6.7	44

#	Article	IF	CITATIONS
55	Development of the Fibrillar and Microfibrillar Structure During Biomimetic Mineralization of Wood. Advanced Functional Materials, 2013, 23, 1265-1272.	14.9	43
56	Fluid adsorption in ordered mesoporous solids determined by in situ small-angle X-ray scattering. Physical Chemistry Chemical Physics, 2010, 12, 7211.	2.8	41
57	Recent Progress in the Replication of Hierarchical Biological Tissues. Advanced Functional Materials, 2013, 23, 4408-4422.	14.9	39
58	A carbon nanopore model to quantify structure and kinetics of ion electrosorption with in situ small-angle X-ray scattering. Physical Chemistry Chemical Physics, 2017, 19, 15549-15561.	2.8	39
59	Nanoporous polymer-derived activated carbon for hydrogen adsorption and electrochemical energy storage. Chemical Engineering Journal, 2022, 427, 131730.	12.7	38
60	Investigation of bone and cartilage by synchrotron scanning-SAXS and -WAXD with micrometer spatial resolution. Journal of Applied Crystallography, 2000, 33, 820-823.	4.5	37
61	Silica replication of the hierarchical structure of wood with nanometer precision. Journal of Materials Research, 2011, 26, 1193-1202.	2.6	37
62	The internal structure of single carbon fibers determined by simultaneous small- and wide-angle scattering. Journal of Applied Crystallography, 2000, 33, 695-699.	4.5	36
63	Evolution of microstructures during dynamic recrystallization and dynamic recovery in hot deformed Nimonic 80a. Materials Science & Engineering A: Structural Materials: Properties, Microstructure and Processing, 2004, 367, 198-204.	5.6	35
64	Nanostructure of Biogenic Calcite Crystals: A View by Small-Angle X-Ray Scattering. Crystal Growth and Design, 2011, 11, 2054-2058.	3.0	35
65	Biological fabrication of cellulose fibers with tailored properties. Science, 2017, 357, 1118-1122.	12.6	35
66	Structural Characterization of Surfactant Aggregates Adsorbed in Cylindrical Silica Nanopores. Langmuir, 2011, 27, 5252-5263.	3.5	33
67	Microporous novolac-derived carbon beads/sulfur hybrid cathode for lithium-sulfur batteries. Journal of Power Sources, 2017, 357, 198-208.	7.8	33
68	Mapping fibre orientation in complex-shaped biological systems with micrometre resolution by scanning X-ray microdiffraction. Micron, 2008, 39, 198-205.	2.2	32
69	Pore lattice deformation in ordered mesoporous silica studied by in situ small-angle X-ray diffraction. Journal of Applied Crystallography, 2007, 40, s522-s526.	4.5	30
70	In-situsmall-angle neutron scattering study of pore filling and pore emptying in ordered mesoporous silica. Journal of Applied Crystallography, 2010, 43, 1-7.	4.5	29
71	Pore-lattice deformations in ordered mesoporous matrices: experimental studies and theoretical analysis. Physical Chemistry Chemical Physics, 2010, 12, 11267.	2.8	29
72	In Situ Measurement of Electrosorption-Induced Deformation Reveals the Importance of Micropores in Hierarchical Carbons. ACS Applied Materials & Interfaces, 2017, 9, 23319-23324.	8.0	29

OSKAR PARIS

#	Article	IF	CITATIONS
73	Influence of Cr23C6 carbides on dynamic recrystallization in hot deformed Nimonic 80a alloys. Materials Science & Engineering A: Structural Materials: Properties, Microstructure and Processing, 2003, 358, 44-51.	5.6	28
74	Pore Structure and Fluid Sorption in Ordered Mesoporous Silica. II. Modeling. Journal of Physical Chemistry C, 2009, 113, 15211-15217.	3.1	28
75	Comparing pore structure models of nanoporous carbons obtained from small angle X-ray scattering and gas adsorption. Carbon, 2019, 152, 416-423.	10.3	28
76	Curvature-induced excess surface energy of fullerenes: Density functional theory and Monte Carlo simulations. Physical Review B, 2010, 81, .	3.2	27
77	3D Printing of Hierarchical Porous Silica and αâ€Quartz. Advanced Materials Technologies, 2018, 3, 1800060.	5.8	27
78	Breaking of Rotational Symmetry during Decomposition of Elastically Anisotropic Alloys. Physical Review Letters, 1995, 75, 3458-3461.	7.8	25
79	Calcium Phosphate with a Channel-like Morphology by Polymer Templating. Chemistry of Materials, 2009, 21, 1572-1578.	6.7	25
80	Elastic properties of graphene obtained by computational mechanical tests. Europhysics Letters, 2013, 103, 68004.	2.0	25
81	Small-Angle Scattering of S-Layer Metallization. Advanced Materials, 2006, 18, 915-919.	21.0	24
82	Cross-sectional texture of carbon fibres analysed by scanning microbeam X-ray diffraction. Journal of Applied Crystallography, 2001, 34, 473-479.	4.5	23
83	Relationship Between Pore Structure and Sorption-Induced Deformation in Hierarchical Silica-Based Monoliths. Zeitschrift Fur Physikalische Chemie, 2015, 229, 1189-1209.	2.8	23
84	Local microstructure and its influence on precipitation behavior in hot deformed Nimonic 80a. Acta Materialia, 2003, 51, 4149-4160.	7.9	21
85	Humidity-driven deformation of ordered mesoporous silica films. Bioinspired, Biomimetic and Nanobiomaterials, 2014, 3, 183-190.	0.9	21
86	The effects of water uptake on mechanical properties of viscose fibers. Cellulose, 2015, 22, 2777-2786.	4.9	21
87	Structure and mechanical properties of carbon fibres: a review of recent microbeam diffraction studies with synchrotron radiation. Journal of Synchrotron Radiation, 2005, 12, 758-764.	2.4	19
88	Hierarchically Organized and Anisotropic Porous Carbon Monoliths. Chemistry of Materials, 2020, 32, 3944-3951.	6.7	19
89	Analysis of pore structure and gas adsorption in periodic mesoporous solids by in situ small-angle X-ray scattering. Colloids and Surfaces A: Physicochemical and Engineering Aspects, 2010, 357, 3-10.	4.7	16
90	Setting Directions: Anisotropy in Hierarchically Organized Porous Silica. Chemistry of Materials, 2017, 29, 7969-7975.	6.7	16

#	Article	IF	CITATIONS
91	The influence of drying and calcination on surface chemistry, pore structure and mechanical properties of hierarchically organized porous silica monoliths. Microporous and Mesoporous Materials, 2019, 288, 109578.	4.4	16
92	The role of topology and thermal backbone fluctuations on sacrificial bond efficacy in mechanical metalloproteins. New Journal of Physics, 2014, 16, 013003.	2.9	15
93	Cantilever bending based on humidity-actuated mesoporous silica/silicon bilayers. Beilstein Journal of Nanotechnology, 2016, 7, 637-644.	2.8	15
94	Nanofibers versus Nanopores: A Comparison of the Electrochemical Performance of Hierarchically Ordered Porous Carbons. ACS Applied Energy Materials, 2019, 2, 5279-5291.	5.1	15
95	Pore characteristics and mechanical properties of silica templated by wood. Bioinspired, Biomimetic and Nanobiomaterials, 2014, 3, 160-168.	0.9	14
96	Transparent cellulose sheets as synthesis matrices for inorganic functional particles. Carbohydrate Polymers, 2012, 87, 257-264.	10.2	13
97	Considerations on the model-free shape retrieval of inorganic nanocrystals from small-angle scattering data. Journal of Applied Crystallography, 2015, 48, 857-868.	4.5	13
98	Towards Real-Time Ion-Specific Structural Sensitivity in Nanoporous Carbon Electrodes Using In Situ Anomalous Small-Angle X-ray Scattering. ACS Applied Materials & Interfaces, 2019, 11, 42214-42220.	8.0	13
99	Diffracting "stacks of cardsâ€⊷ some thoughts about small-angle scattering from bone. , 2005, , 33-39.		12
100	Apparent lattice expansion in ordered nanoporous silica during capillary condensation of fluids. Journal of Applied Crystallography, 2012, 45, 798-806.	4.5	12
101	Quantifying adsorption-induced deformation of nanoporous materials on different length scales. Journal of Applied Crystallography, 2017, 50, 1404-1410.	4.5	12
102	Mechanical Characterization of Hierarchical Structured Porous Silica by in Situ Dilatometry Measurements during Gas Adsorption. Langmuir, 2019, 35, 2948-2956.	3.5	12
103	Repeated sorption of water in SBA-15 investigated by means of <i>in situ</i> small-angle x-ray scattering. Journal of Physics Condensed Matter, 2012, 24, 284112.	1.8	11
104	Deformation mechanism of nanoporous materials upon water freezing and melting. Applied Physics Letters, 2012, 101, .	3.3	11
105	The pomelo peel and derived nanoscale-precision gradient silica foams. Bioinspired, Biomimetic and Nanobiomaterials, 2012, 1, 117-122.	0.9	11
106	The structural evolution of multi-layer graphene stacks in carbon fibers under load at high temperature – A synchrotron radiation study. Carbon, 2014, 80, 373-381.	10.3	11
107	In Situ Small-Angle Neutron Scattering Investigation of Adsorption-Induced Deformation in Silica with Hierarchical Porosity. Langmuir, 2019, 35, 11590-11600.	3.5	11
108	Reversibly compressible and freestanding monolithic carbon spherogels. Carbon, 2019, 153, 189-195.	10.3	11

#	Article	IF	CITATIONS
109	Hierarchical Architectures to Enhance Structural and Functional Properties of Brittle Materials. Advanced Engineering Materials, 2017, 19, 1600683.	3.5	10
110	Structural analysis of Gossypium hirsutum fibers grown under greenhouse and hydroponic conditions. Journal of Structural Biology, 2016, 194, 292-302.	2.8	9
111	SANS investigation of phase separation in hot-deformed Nimonic 80a. Scripta Materialia, 2002, 47, 25-30.	5.2	8
112	Development of foam-like emulsion phases in porous media flow. Journal of Colloid and Interface Science, 2022, 608, 1064-1073.	9.4	8
113	Mapping Lattice Spacing and Composition in Biological Materials by Means of Microbeam Xâ€Ray Diffraction. Advanced Engineering Materials, 2011, 13, 784-792.	3.5	7
114	Pore shape and sorption behaviour in mesoporous ordered silica films. Journal of Applied Crystallography, 2016, 49, 1713-1720.	4.5	7
115	Plasma-Derived Graphene-Based Materials for Water Purification and Energy Storage. Journal of Carbon Research, 2019, 5, 16.	2.7	7
116	Hybrid carbon spherogels: carbon encapsulation of nano-titania. Chemical Communications, 2021, 57, 3905-3908.	4.1	7
117	Separation of scattering contributions from carbides and Î ³ ' precipitates in Nimonic 80a by combining small-angle X-ray and neutron scattering. Journal of Applied Crystallography, 2003, 36, 484-488.	4.5	6
118	Nanomechanical studies of the compressive behavior of carbon fibers. Journal of Materials Science, 2010, 45, 6845-6848.	3.7	6
119	Passive and active mechanical properties of biotemplated ceramics revisited. Bioinspiration and Biomimetics, 2016, 11, 065001.	2.9	6
120	CHAPTER 8. The Mineralized Crustacean Cuticle: Hierarchical Structure and Mechanical Properties. RSC Smart Materials, 2013, , 180-196.	0.1	5
121	Complementary High Spatial Resolution Methods in Materials Science and Engineering. Advanced Engineering Materials, 2017, 19, 1600671.	3.5	5
122	Adsorption-induced deformation of hierarchical organised carbon materials with ordered, non-convex mesoporosity. Molecular Physics, 2021, 119, .	1.7	5
123	A new device for high-temperature <i>in situ</i> GISAXS measurements. Review of Scientific Instruments, 2018, 89, 035103.	1.3	4
124	Hierarchically organized materials with ordered mesopores: adsorption isotherm and adsorption-induced deformation from small-angle scattering. Physical Chemistry Chemical Physics, 2020, 22, 12713-12723.	2.8	4
125	Capillary bridge formation between hexagonally ordered carbon nanorods. Adsorption, 2020, 26, 563-578.	3.0	4
126	Microcracks in Carbon/Carbon Composites: A Microtomography Investigation using Synchrotron Radiation. Materials Research Society Symposia Proceedings, 2001, 678, 381.	0.1	3

#	Article	IF	CITATIONS
127	Shell-Models for Multi-Layer Carbon Nano-Particles. Advanced Structured Materials, 2011, , 585-602.	0.5	3
128	A Facile Oneâ€Pot Synthesis of Hierarchically Organized Carbon/TiO ₂ Monoliths with Ordered Mesopores. ChemPlusChem, 2021, 86, 275-283.	2.8	3
129	Some introductory remarks on microbeam diffraction in nanobiosciences. Journal of Synchrotron Radiation, 2005, 12, 712-712.	2.4	2
130	Small-angle scattering from spherical particles on randomly oriented interfaces. International Journal of Materials Research, 2006, 97, 290-294.	0.8	1
131	Bioinspired composites – next generation of materials and devices. Bioinspired, Biomimetic and Nanobiomaterials, 2014, 3, 121-122.	0.9	1
132	Bowtie-Shaped Deformation Isotherm of Superhydrophobic Cylindrical Mesopores. Langmuir, 2022, 38, 211-220.	3.5	1
133	Water Melting Induced Deformation of Ordered Nanoporous Silica. , 2013, , .		Ο
134	Small-angle scattering from spherical particles on randomly oriented interfaces. International Journal of Materials Research, 2022, 97, 290-294.	0.3	0